

Monte Carlo study of electron transmission and backscattering from metallic thin films

K. L. Hunter,* I. K. Snook, and H. K. Wagenfeld

Applied Physics Department, Royal Melbourne Institute of Technology, Melbourne, Victoria, Australia

(Received 18 December 1995)

A Monte Carlo trajectory model that describes electron transport in semi-infinite metallic solids also gives quantitative agreement with experiment for the transmission fraction for thin films of Be, Al, Cu, and Au and for the energy distribution in Al, both as a function of primary energy E_p and of film thickness t . Significantly, the results enabled the construction of universal curves of transmission and backscattered fractions versus reduced film thickness $t_n = t/\bar{x}_p$ for each element, where \bar{x}_p is the mean depth of penetration of primary electrons in the semi-infinite solids. As \bar{x}_p may also be fitted to empirical curves, these results may be used to predict transmission and backscattering for thin films without future resort to lengthy numerical calculations. [S0163-1829(96)08431-7]

I. INTRODUCTION

Electron transmission, backscattering, and secondary electron emission are very important phenomena involved in a great number of widely used techniques and instruments, for example, electron microscopy, surface electron spectroscopy, and particle detection. Although there is no complete analytical theory of electron scattering and secondary emission by solids, many numerical methods based on the Monte Carlo technique have been very successful in describing various aspects of electron transport.¹⁻⁶ There are many published methods based on this approach that differ largely in the manner of approximating the individual electron collision processes. In a previous paper⁶ we developed such a method to investigate backscattering and secondary electron emission in semi-infinite solids. The method was shown to give a good account of mean depth of penetration of primary electrons, \bar{x}_p , and backscattering fraction, η , and a moderately good qualitative description of secondary electron yield curves for Al.⁷ The method also enabled a description of secondary electron emission from thin layers on substrates.⁷ Furthermore, we were able to give some insight into the importance of the various processes involved in secondary electron emission and to give estimates of quantities such as the mean depth of production of secondaries, which complements information obtainable from experiment.^{6,7}

Because of the importance of solid thin films in such areas as microelectronics, coatings, and transmission electron microscopy we have, in this paper, extended the above-mentioned calculations to study electron transmission and backscattering in several typical thin metal films.

II. METHOD

As the method has been fully detailed in a previous paper⁶ we give only a brief outline and summary of the main ideas involved. We used the quantum-mechanical phase-shift method for calculating the elastic (core) scattering as implemented by Pendry.⁸ The following inelastic collision processes were modelled: the inner-shell excitation was described by the method due to Gryzinski,⁹ the plasmon

excitation was described by the methods of Farrell¹⁰ and Quinn,¹¹ and the single-particle conduction electrons were treated by a combination of experimental mean free paths^{12,13} and the Streitwolf excitation function.¹⁴ Thus, we have ignored the details of the band structure of the metal and, hence, ignored such processes as interband transitions.

In the Monte Carlo (MC) process^{1,6} one chooses, on a random basis, the type of collision and then moves the electron until the next collision a distance determined by the total scattering cross section, i.e., mean free path, for that process. The energy loss (if any), ΔE , is then obtained from the differential cross section as detailed previously. The angle of scattering, Ω , was obtained from either the differential cross section or use of the binary collision model, whichever was appropriate.⁶ This process is continued until the energy of the electron is below a certain preset threshold level or until it has left the solid. Results were generated using a range of values of this threshold energy and it was found that the results were insensitive to the value of this energy for values up to 100 eV.

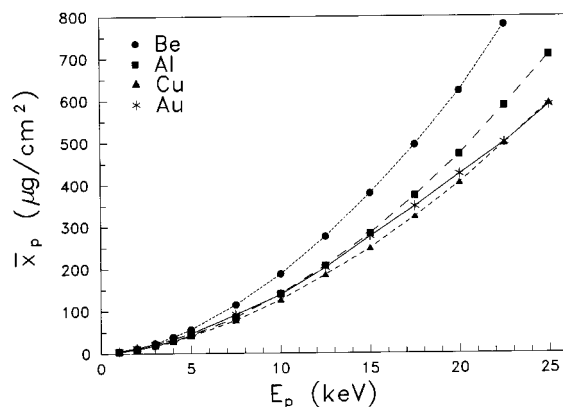


FIG. 1. Mean depth of penetration, \bar{x}_p , for electrons of energy E_p normally incident on Be, Al, Cu, and Au. The dots are the experimental data of Kanya and Kawakatsu (Ref. 15). The lines are empirical fits to the MC data as discussed in the text.

TABLE I. Material-dependent parameters used in the calculation of the scattering cross sections. Z is the atomic number and A the atomic mass of the element, ρ is the mass density, ϕ is the work function, E_f is the Fermi energy, and E_{pl} is the Plasmon energy of the solid.

	Be	Al	Cu	Au
Z	4	13	29	79
A (a.m.u.)	9.01	26.98	63.55	196.97
ρ (g/cm ³)	1.82	2.70	8.92	19.3
ϕ (eV)	4.98	4.28	4.65	5.10
E_f (eV)	14.1	11.63	7.0	5.51
E_{pl} (eV)	18.5	15.8	15.2	12.1

III. RESULTS FOR SEMI-INFINITE SOLIDS

In order to assess the accuracy and limitations of the above method we first simulated Be, Al, Cu, and Au since these span a large range of typical metal parameters (see Table I) and there exists reasonably extensive experimental data with which to compare our simulated results. The calculations were performed for the parameters in Table I using 25,000 individual primary electron trajectories.

The mean depth of penetration of the primary electrons \bar{x}_p is in excellent agreement with experiment;¹⁵ see Fig. 1. Although we found \bar{x}_p cannot be fitted by Eq. 1,

$$\bar{x}_p = A E_p^n, \quad (1)$$

which is often used in ion scattering studies, we could fit the data to the form (1) over restricted energy ranges, $0 < E_p < 1.5$ keV, $1.5 \text{ keV} < E_p < 5$ keV, and $5 \text{ keV} < E_p < 25$ keV using different values of A and n , which we call A_1, A_2 , and A_3 , and n_1, n_2 , and n_3 , respectively; see Table II. These provide a convenient fit to the Monte Carlo data for use in such areas as surface electron spectroscopy and electron microscopy, and in the description of thin films in Sec. IV.

The calculated values of the backscattering coefficient η are in reasonable agreement with experiment,¹⁶ see Fig. 2, particularly for $E_p > 5$ keV, which seems to be typical of most MC studies.^{1,2,6} Interestingly, the MC results for the mean relative backscattering electron energy, \bar{E}_{bs}/E_p , showed little variation with E_p , ranging from about 0.8 for Au, 0.7 for Cu, 0.65 for Al, to 0.55 for Be. Also, the mean depth of penetration of the backscattered electrons, \bar{x}_{bs} , as a function of E_p , was found to very nearly obey the approximate relation

$$\bar{x}_{bs} = k \bar{x}_p, \quad (2)$$

TABLE II. Calculated values of $A_{1..3}$ and $n_{1..3}$ used in Eq. (1) to describe the penetration of electrons into Be, Al, Cu, and Au.

	Be	Al	Cu	Au
A_1	200.0	140.0	43.0	26.0
n_1	1.0	1.0	1.0	1.0
A_2	203.0	121.5	40.0	24.0
n_2	1.69	1.60	1.50	1.45
A_3	193.0	95.5	30.8	19.6
n_3	1.74	1.74	1.67	1.58

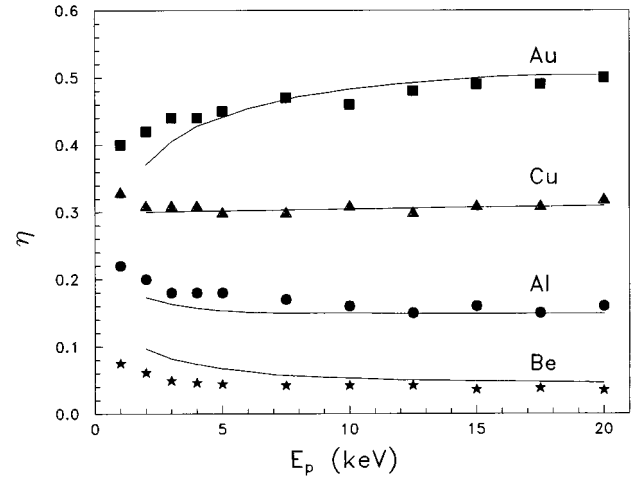


FIG. 2. Electron backscattering coefficient, η , from targets of Be, Al, Cu, and Au. The solid lines are the experimental results of Reimer and Tollkamp.¹⁶

with k being about 0.4 except for Be, which is lower (about 0.3), most likely due to the relatively stronger inelastic scattering in Be resulting in a lower probability for primary electrons being scattered back to the surface from deeper within the solid.

IV. RESULTS FOR THIN FILMS

We applied the method described above to thin films of Be, Al, Cu, and Au for a range of thicknesses t .

The results for the transmission fraction η_t as a function of normalized film thickness t_n , defined by

$$t_n = t/\bar{x}_p, \quad (3)$$

are shown for Al in Fig. 3 for $E_p = 1, 3$, and 10 keV, and as can be seen the results are in good agreement with experiment^{17,18} and, furthermore, form a universal curve which is independent of E_p . Similar results were obtained for Be, Cu, and Au and the collected results may be seen in

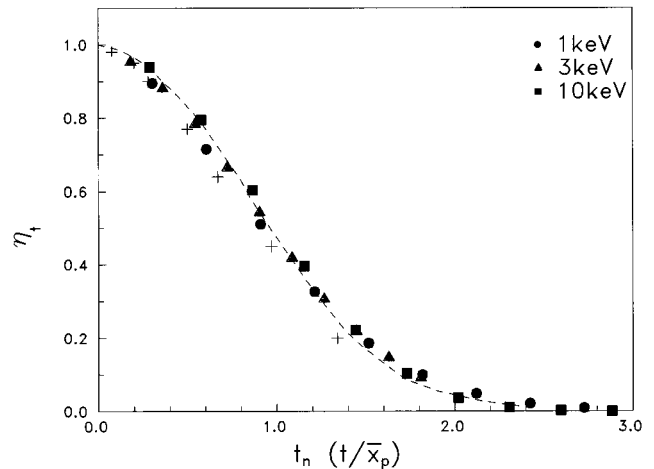


FIG. 3. Transmission fraction η_t of electrons through Al as a function of the normalized film thickness, t_n , for incident electrons of 1, 3, and 10 keV. The dashed line and the pluses are experimental results from Refs. 17 and 18, respectively.

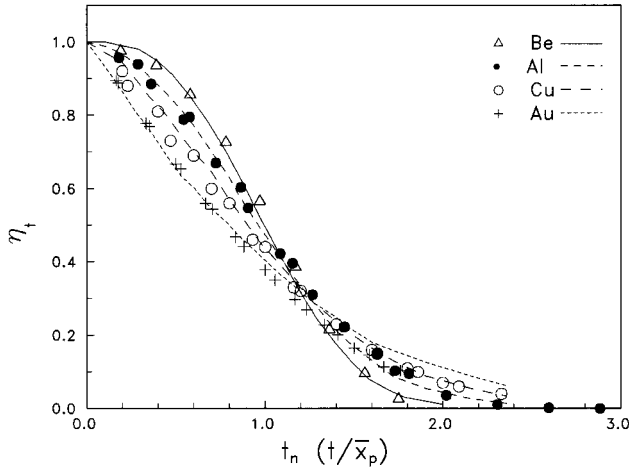


FIG. 4. Monte Carlo results for η_t through targets of Be, Al, Cu, and Au as a function of t_n . The lines are the experimental data of Vyatskin and Trunev¹⁷ for Al, Cu, and Au and of Fitting¹⁹ for Be.

Fig. 4 compared with experimental results.^{17,19} These curves should prove to be of use in calculating the intensity of transmission through thin films, e.g., in electron microscopy, and in studying electron enhanced adhesion.²⁰

In Fig. 5 we show the MC results for the energy distribution of electrons transmitted through thin films of Al as a function of t_n for $E_p = 5$ keV. As can be seen, there is good agreement with experiment,¹⁹ and as t_n is increased, the energy distribution of the transmitted electrons becomes less peaked and the mean energy moves towards lower values. Similar results were obtained for E_p between 1 and 20 keV and are, thus, not shown here. Once again the good agreement with experiment shows that the method is of potential use in interpreting intensity data in electron microscopy and electron-beam-enhanced adhesion.²⁰

The results for the backscattering coefficient of thin films, η_f , are reduced from that of the corresponding semi-infinite target η , when the thickness of the film becomes less than the maximum depth reached by primary electrons. This is shown in Fig. 6 for the extreme cases of Be and Au for E_p 's

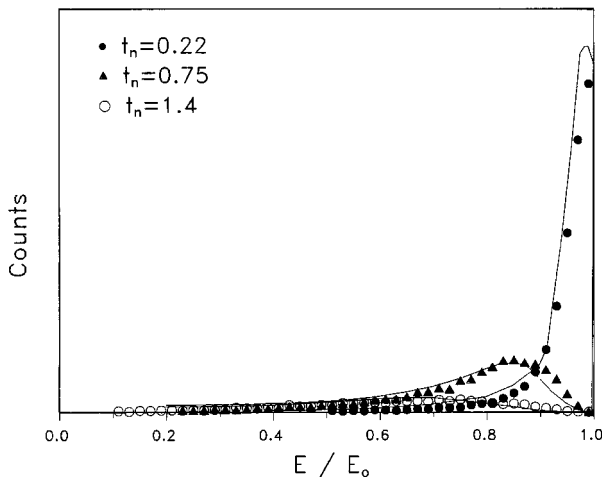


FIG. 5. Energy distribution of electrons transmitted through thin films of Al with normalized thicknesses of $t_n = 0.22, 0.75,$ and 1.4 . The solid lines are the experimental data of Fitting.¹⁹

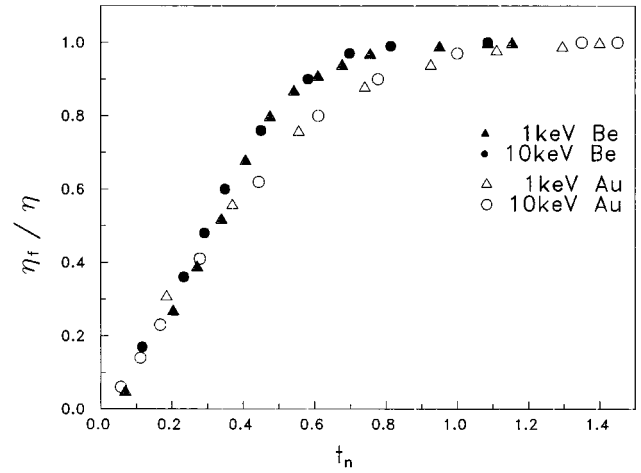


FIG. 6. Relative backscattering fraction from thin films of Be and Au plotted against the normalized film thickness, t_n , at incident energies of 1 and 10 keV.

of 1 and 10 keV. The result indicate that one must take into account the thickness of the film on the backscattering coefficient in any application using thin films. Interestingly, the relative values, i.e., η_t / η plotted against t_n , show very little variation with the element involved or primary electron energy in the range used in this study, once again indicating potentially useful scaling relationships.

Analogous scaling relationships have previously been discovered for positron implantation profiles $P(z)$ (and for electrons in Cu and Au) in semi-infinite solids.²² Our scaling results are a generalization of these as, although one can deduce approximate values of $P(z)$ from η_t and η_f using²³

$$P(z) \approx -d\eta_t/dz - d\eta_f/dz, \quad (4)$$

one clearly cannot deduce η_t and η_f from $P(z)$ alone. Thus, while the scaling relation for $P(z)$ can be deduced from those for η_t and η_f , the converse is not possible.

Furthermore, one not only needs both η_t and η_f to describe scattering in thin films but, unlike $P(z)$, η_t and η_f are functions of film thickness as well as of E_p , hence our scaling results are more general than those obtained previously.²²

V. CONCLUSIONS

In this paper we have shown that a Monte Carlo model previously successfully used to describe electron transport in semi-infinite solids and thin films on thick substrates was able to give a quantitative description of electron transmission in a wide variety of metallic thin films. The method also gave a good description of the energy distribution of electrons transmitted through thin aluminium films.

Furthermore, the results show that for a given element the transmitted fraction η_t may be expressed as universal functions of the reduced film thickness $t_n = t / \bar{x}_p$, where \bar{x}_p is the mean depth of penetration of primary electrons in the semi-infinite solid. Similarly, the calculated backscattered fractions, η also obeys similar scaling relations. As \bar{x}_p may be fitted to simple equations (see Sec. II), then these relationships are of potential use for calculating η_t and η for metallic thin films without having to repeat lengthy MC calcula-

tions for different thicknesses and primary energies. These relationships are, therefore, of potential use in transmission-electron microscopy and electron-enhanced adhesion studies.

As mentioned in the previous section, an analogous scaling relationship has previously been discovered for positron implantation profiles in semi-infinite solids.²² However, to describe implantation in a semi-infinite solid one only needs $P(z)$ as a function of primary energy E_p , but for scattering from a thin film one needs both η_t and η_f as a function of E_p and film thickness t . Hence our results provide an extension of previous results to electrons and to thin films.

It is interesting to speculate as to why these scaling relationships occur. A possible answer lies in the work of Shimizu and Ding¹ and of Gauvin and Drouin,²¹ who have shown that the electron trajectories and their distribution within the interaction volume obey fractal scaling laws. Thus, the scattering volume and its shape, although altering with the incident energy, is self-similar, i.e., the results from one simulation can, in principle, be used to predict those for another simulation of the same element by an appropriate scaling of the results of the first simulation.

*Current address, ETP Instruments PTY. Ltd., Sydney, Australia.

¹R. Shimizu and Ding Ze-Jun, Rep. Prog. Phys. **55**, 487 (1992).

²M. Yasuda, H. Kawata, and K. Murata, J. Appl. Phys. **77**, 4706 (1995).

³S. Valkealahti and R. M. Nieminen, Appl. Phys. A **32**, 95 (1983); **35**, 51 (1984).

⁴M. Dapor, Phys. Rev. B **46**, 618 (1992).

⁵G. R. Massoumi, W. N. Lennard, H. H. Jorch, and P. J. Schultz, in *Positron Beams for Solids and Surfaces*, AIP Conf. Proc. No. 218 (American Institute of Physics, New York, 1990), p. 40.

⁶K. L. Hunter, I. K. Snook, D. L. Swingler, and H. K. Wagenfeld, J. Phys. D. **23**, 1738 (1990).

⁷K. L. Hunter, I. K. Snook, and H. K. Wagenfeld, J. Phys. D. **27**, 1769 (1994).

⁸J. P. Pendry, *Low Energy Electron Diffraction* (Academic, New York, 1974).

⁹M. Gryzinski, Phys. Rev. **138A**, 305 (1965).

¹⁰R. A. Farrell, Phys. Rev. **107**, 450 (1957).

¹¹J. J. Quinn, Phys. Rev. **126**, 453 (1962).

¹²M. P. Sear and W. A. Dench, Surf. Inter. Anal. **1**, 2 (1979).

¹³S. Tanuma, C. J. Powell, and D. R. Penn, Surf. Inter. Anal. **11**, 577 (1988).

¹⁴H. W. Streitwolf, Ann. Phys. (Leipzig) **3**, 183 (1959).

¹⁵K. Kanaya and K. Kawakatsu, J. Phys. D **5**, 1727 (1972).

¹⁶L. Reimer and C. Tollkamp, Scanning **3**, 35 (1980).

¹⁷A. Ya Vyatskin and V. V. Trunev, Radio Eng. Electron. Phys. **12**, 1526 (1967).

¹⁸K. O. Al-Ahmad and D. E. Watt, J. Phys. D **16**, 2257 (1983).

¹⁹H.-J. Fitting, Phys. Status Solidi A **26**, 525 (1974).

²⁰M. Tay, J. Gazecki, M. D. McCubbery, and J. S. Williams, Nucl. Instrum. Methods Phys. Res. B **43**, 379 (1990); S. D. Moss, R. A. O'Sullivan, P. J. K. Paterson, I. K. Snook, A. J. Russo, A. Katsaros, and N. Savvides, J. Appl. Phys. **78**, 5782 (1995).

²¹R. Gauvin and D. Drouin, Scanning **14**, 313 (1992).

²²V. J. Ghosh and G. C. Aers, Phys. Rev. B **51**, 45 (1995); V. J. Ghosh, M. McKeown, D. O. Welch, and K. G. Lynn, Nucl. Instrum. Methods Phys. Res. B **90**, 442 (1994); G. C. Aers, J. Appl. Phys. **76**, 1622 (1994); P. A. Huttunen, J. Makinen, and A. Veranen, Phys. Rev. **41**, 8062 (1990).

²³S. Valkealahti and R. M. Nieminen, Appl. Phys. **32**, 95 (1983); H. E. Hansen and U. Ingerslev-Jensen, J. Phys. D **16**, 1353 (1983).